

Title	Crack Propagation Analysis Using Interface Element (Report I) : Theoretical Formulation and Potential Fields of Application(Mechanics, Strength & Structure Design)
Author(s)	Murakawa, Hidekazu; Serizawa, Hisashi; Wu, Zhengqi
Citation	Transactions of JWRI. 27(2) P.67-P.72
Issue Date	1998-12
Text Version	publisher
URL	http://hdl.handle.net/11094/3690
DOI	
rights	本文データはCiNiiから複製したものである
Note	

Osaka University Knowledge Archive : OUKA

<https://ir.library.osaka-u.ac.jp/repo/ouka/all/>

Crack Propagation Analysis Using Interface Element (Report I) †

- Theoretical Formulation and Potential Fields of Application -

Hidekazu MURAKAWA*, Hisashi SERIZAWA** and Zhengqi Wu***

Abstract

Fiber reinforced composite materials and the composites with a thin film coating are applied in various fields as structural materials because of their high specific strength and stiffness which contribute to weight savings. The conventional materials, such as metals and ceramics, are also used under severe conditions due to the recent improvement of their performances. From the point of view of safe design of the structures, it is very important to estimate the fracture strength of materials with a reasonable accuracy. Many methods to evaluate the failure strength of materials have been proposed. There are basically two approaches. One is the macroscopic approach in which the concepts of stress intensity factor, energy release rate and J-integral are employed. The other is the microscopic approach such as the simulation of crack propagation using molecular dynamics¹⁾. To evaluate the strength of a structural component, both the macroscopic and the microscopic nature of the phenomena must be taken into account. It is also noted that problems, such as ductile crack growth in metals and brittle fracture of ceramics and composite materials, are highly nonlinear and time dependent. Thus, extremely heavy computation is required. In addition, the mechanisms of crack extension or interface stripping have not been thoroughly clarified.

In this study, a new and simple method is developed in order to simulate the fracture phenomena that can be considered as the formation of new surface as a result of crack propagation. Based on the fact that surface energy must be supplied for the formation of new surface, a potential function representing the surface energy density is introduced in the finite element method. The proposed method is applied to the mode-I and II crack propagation problems and its capability for static and dynamic analyses is demonstrated.

KEY WORDS: (Interface element) (Interface potential) (Peeling test) (Push-out test) (Dynamic crack propagation) (Ductile crack propagation)

1. Introduction

The phenomena of crack propagation and interface stripping can be regarded as the formation of a new surface. Thus, it is quite natural to model these problems by introducing the mechanism of surface formation. The authors proposed a method in which the formation of new surface is represented by interface element based on the interface potential energy²⁾. The general idea of the interface element and its application to peeling test of film³⁾, push-out test of fiber in matrix⁴⁾, dynamic crack propagation⁵⁾, and ductile tearing of steel plate are presented in this report.

2. Method of Analysis

2.1 Surface potential

Figure 1 shows an illustration of the crack

propagation modeled using interface elements. The interface element consists of two surfaces and it has no

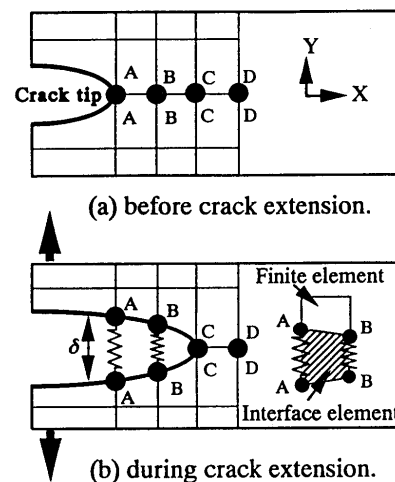


Fig.1 Crack propagation model with interface element.

† Received on December 7, 1998

* Associate Professor

** Research Associate

*** Graduate Student, Osaka University

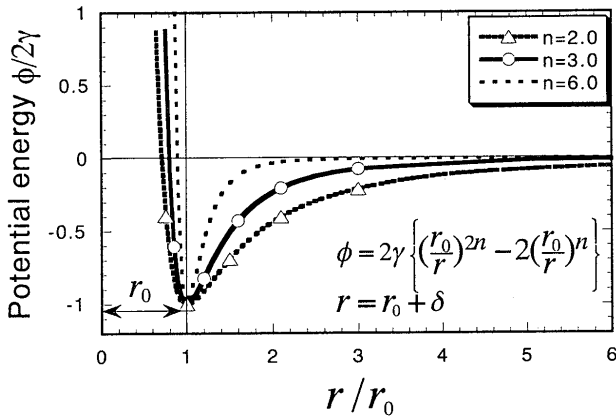


Fig.2 Lennard-Jones type interface potential.

thickness when the load is not acting. When the load is applied, the two surfaces separate from each other. The distance between the surfaces, or the crack opening, is denoted by δ . The mechanical characteristics of the interface element are defined through a potential function $\phi(\delta)$. Since the function $\phi(\delta)$ can be chosen rather arbitrarily, the Lennard-Jones type potential energy⁶⁾ described by the following equation is employed in this study.

$$\phi(\delta) = 2\gamma \cdot \left\{ \left(\frac{r_0}{r_0 + \delta} \right)^{2n} - 2 \cdot \left(\frac{r_0}{r_0 + \delta} \right)^n \right\} \quad (1)$$

Where δ is the crack opening and γ , n and r_0 are the material constants. In particular, 2γ is the surface energy per unit area. As shown in Fig.2, n controls the shape of the potential energy. The derivative of ϕ with respect to δ gives the bonding force per unit area of the surface. As shown in Fig.3, the bonding force rapidly decreases with increasing δ . Through this phenomenon, the formation of new surface can be described.

2.2 Equilibrium equation of system

For simplicity, the outline of the mathematical formulation is presented using the crack propagation problem in an elastic solid. When the material is elastic, the equilibrium equation can be derived based on the principle of minimum potential energy.

The total energy Π of an elastic body with a propagating crack can be described as the sum of the strain energy U , and the potential of the external load W and the interface energy for the newly formed surface during crack propagation U_s , ie.

$$\Pi = U + U_s + W \quad (2)$$

In case of the finite element method, the elastic body to be analyzed is subdivided into small elements and the displacements in each element are interpolated by nodal displacement u_0 . Noting this, the total energy is

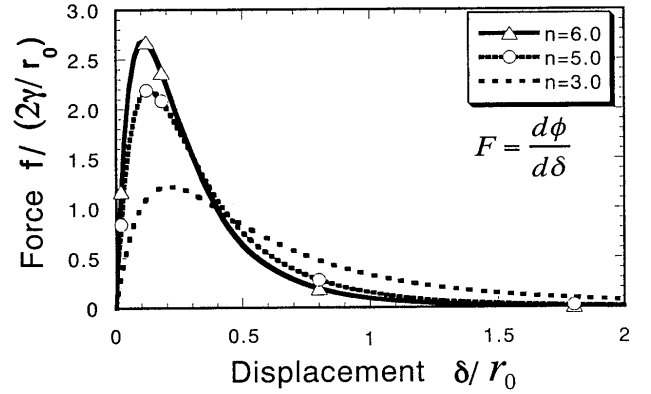


Fig.3 Bonding force acting on interface.

described as,

$$\Pi = \Pi(u_0) = U(u_0) + U_s(u_0) + W(u_0) \quad (3)$$

Further, $U(u_0)$, $U_s(u_0)$ and $W(u_0)$ can be represented as the sum of the contributions from each element $U^e(u_0^e)$, $U_s^e(u_0^e)$ and $W^e(u_0^e)$, ie.

$$\Pi(u_0) = \sum \{ U^e(u_0^e) + U_s^e(u_0^e) + W^e(u_0^e) \} \quad (4)$$

where, u_0^e is the nodal displacement vector for each element extracted from the nodal displacement vector of the whole system u_0 .

Once the total energy Π is given as in Eq.(4), the equilibrium equation in incremental form can be derived in the following manner. Denoting the nodal displacement at the present step and its increment to the next step as u_0 and Δu_0 , the total energy Π can be described as a function of $u_0 + \Delta u_0$ and it can be expanded into Taylor's series, ie.

$$\begin{aligned} \Pi(u_0 + \Delta u_0) &\approx \Pi(u_0) + \Delta^1 \Pi(\Delta u_0) + \Delta^2 \Pi(\Delta u_0) \\ &= \Pi(u_0) - \{ \Delta u_0 \}^T \{ f \} + \frac{1}{2} \cdot \{ \Delta u_0 \}^T [k] \{ \Delta u_0 \} \end{aligned} \quad (5)$$

where, $\Delta^1 \Pi$ and $\Delta^2 \Pi$ are the first and the second terms in Δu_0 , ie.

$$\Delta^1 \Pi(\Delta u_0) = -\{ \Delta u_0 \}^T \{ f \} \quad (6)$$

$$\Delta^2 \Pi(\Delta u_0) = \frac{1}{2} \cdot \{ \Delta u_0 \}^T [k] \{ \Delta u_0 \} \quad (7)$$

Further, the equilibrium equation can be derived as the stationarity condition of $\Pi(u_0 + \Delta u_0)$ with respect to Δu_0 , ie.

$$\frac{\partial \Pi(u_0 + \Delta u_0)}{\partial \Delta u_0} = -\{ f \} + [k] \{ \Delta u_0 \} = 0 \quad (8)$$

or,

$$[k] \{ \Delta u_0 \} = \{ f \} \quad (9)$$

where, $[k]$ and $\{ f \}$ are the tangent stiffness matrix and the load vector, respectively.

2.3 Stiffness matrix and force vector of interface element

The stiffness matrix and the load vector of the interface element can be derived in a manner basically similar to that for the whole system. Since the FEM code developed in this research is a three dimensional code using a solid element, the same 8-node solid element is used for the interface element as shown in **Fig.4**. The interface element consists of two surfaces containing four nodes, namely nodes 1-4 for the bottom surface and 5-8 for the top surface, and it has no thickness when load is not applied. The two surfaces separate when the load is applied and the distance or the opening is denoted by δ . When the surface area of the interface element is S^e , the interface energy for an element $U_s^e(u_0^e)$ is given by the following equation.

$$U_s^e(u_0^e) = \int \phi(\delta) \cdot dS^e \quad (10)$$

where, δ is the opening at an arbitrary point on the surface and it can be interpolated using the interpolation function $N_i(\xi, \eta)$, ie.

$$\delta(\xi, \eta) = \sum N_i(\xi, \eta) \cdot (w_{i+4} - w_i) \quad (11)$$

where,

$$N_1(\xi, \eta) = 0.25 \cdot (1 + \xi) \cdot (1 - \eta) \quad (12)$$

$$N_2(\xi, \eta) = 0.25 \cdot (1 + \xi) \cdot (1 + \eta) \quad (13)$$

$$N_3(\xi, \eta) = 0.25 \cdot (1 - \xi) \cdot (1 + \eta) \quad (14)$$

$$N_4(\xi, \eta) = 0.25 \cdot (1 - \xi) \cdot (1 - \eta) \quad (15)$$

and w_i is the nodal displacement normal to the surface.

Finally, the stiffness matrix $[k^e]$ and the load vector $\{f^e\}$ of the interface element can be derived by expanding $U_s^e(u_0^e + \Delta u_0^e)$ with respect to Δu_0^e in the following manner.

$$U_s^e(u_0^e + \Delta u_0^e) = \int \phi(\delta + \Delta \delta) \cdot dS^e$$

$$= \int \phi(\delta) \cdot dS^e + \int \frac{d\phi(\delta)}{d\delta} \cdot \frac{\partial \delta}{\partial u_0^e} \cdot \Delta u_0^e \cdot dS^e + \frac{1}{2} \cdot \int \frac{d^2\phi(\delta)}{d\delta^2} \cdot \left(\frac{\partial \delta}{\partial u_0^e} \cdot \Delta u_0^e \right)^2 \cdot dS^e + H.O.T. \quad (16)$$

where,

$$\int \frac{d\phi(\delta)}{d\delta} \cdot \frac{\partial \delta}{\partial u_0^e} \cdot \Delta u_0^e \cdot dS^e = -\{f^e\}^T \{\Delta u_0^e\} \quad (17)$$

$$\frac{1}{2} \cdot \int \frac{d^2\phi(\delta)}{d\delta^2} \cdot \left(\frac{\partial \delta}{\partial u_0^e} \cdot \Delta u_0^e \right)^2 \cdot dS^e = \frac{1}{2} \cdot \{\Delta u_0^e\}^T [k^e] \{\Delta u_0^e\} \quad (18)$$

Since the interface element has no volume or mass, the same formulation can be applied to both the static and the dynamic problems. Further, by arranging the interface elements along the crack extension path in the ordinary FEM model, crack propagation problems can be analyzed.

3. Simulation of Peeling Test

Figure 5 shows the peeling test to be analyzed by the proposed method. The computed load-displacement curves are shown in **Figs.6-9**. The computed results show that the crack starts to propagate at the maximum load. Then, the load gradually decreases with increase of peeling length. **Figures 6 and 7** show the effect of material constants r_0 and n . It is seen that the force at the start of crack extension becomes large when r_0 is small or n is large, while the curve during the crack propagation is not influenced by r_0 or n . **Figure 8** shows that the value of γ influences both the initiation and the crack extension. These results suggest that crack extension in the peeling test is primarily governed by the magnitude of the surface energy γ . The effect of mesh size is examined in **Fig.9**. As seen from the figure, the mesh size does not show any significant effect on the load-displacement curve. Further, the peeling problem of wider films as shown in **Fig.10** is simulated to demonstrate the potential versatility of the proposed method.

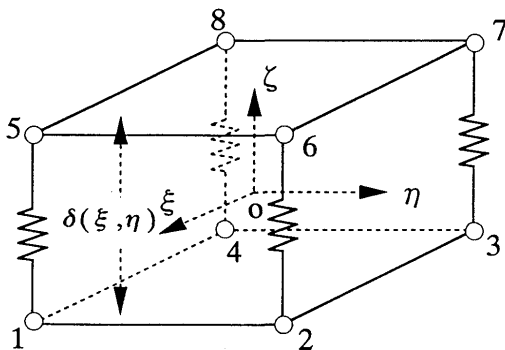


Fig.4 Interface element and interpolation of crack opening.

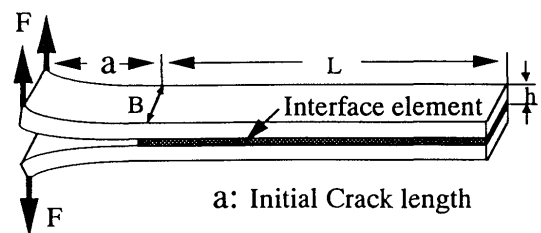


Fig.5 Peeling test model for FEM analysis.

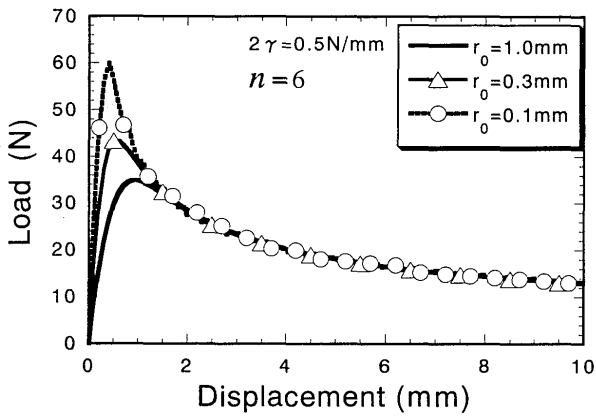


Fig.6 Effect of r_0 on load-displacement curve.

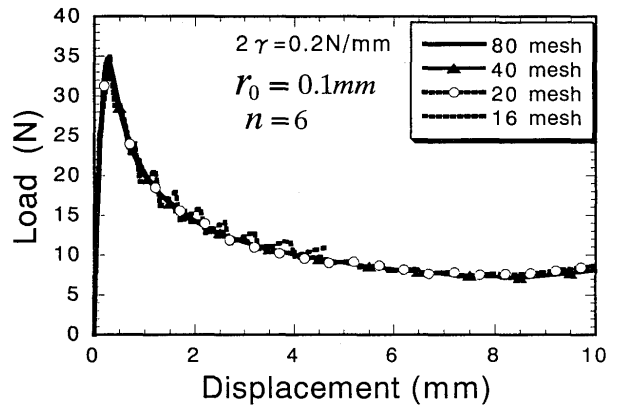


Fig.9 Effect of mesh division on load-displacement curve.

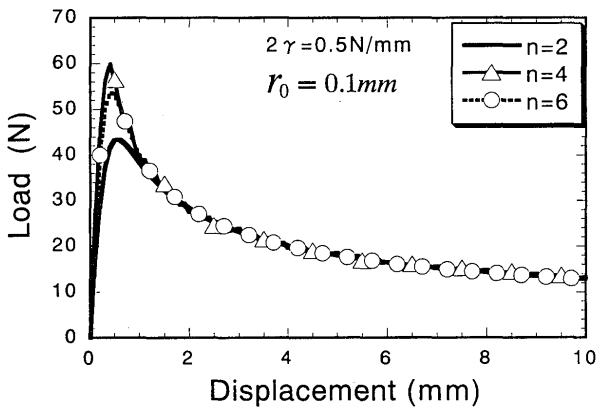


Fig.7 Effect of n on load-displacement curve.

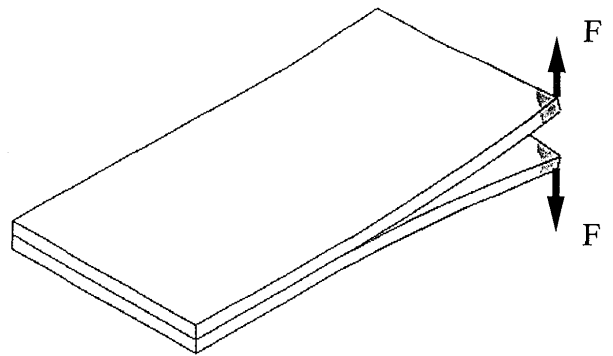


Fig.10 Peeling of wide films.

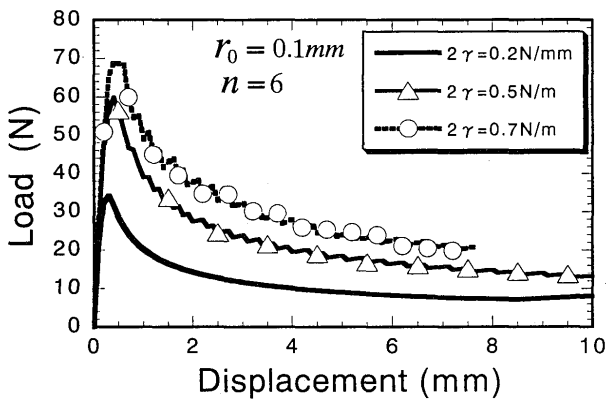


Fig.8 Effect of γ on load-displacement curve.

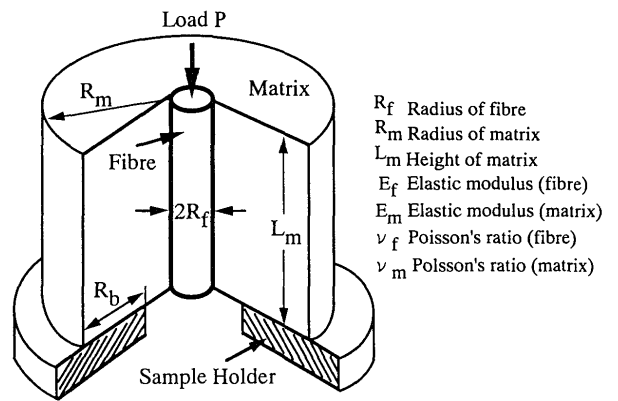


Fig.11 Model for push-out test of fiber in matrix.

4. Push-out Test of Fiber in Matrix

The proposed method can be applied also to mode-II crack propagation problems with minor modification. The push-out test of a fiber in matrix shown in Fig.11 is analyzed. The computed load-displacement curves are presented in Fig.12. The relatively horizontal part after the linear stage corresponds to the crack propagation process. This means the load is almost constant during the crack propagation. The sudden drop of the load observed in the case of $2\gamma = 0.2 \text{ N/mm}$ represents the moment when the interface crack reaches the bottom surface of the matrix.

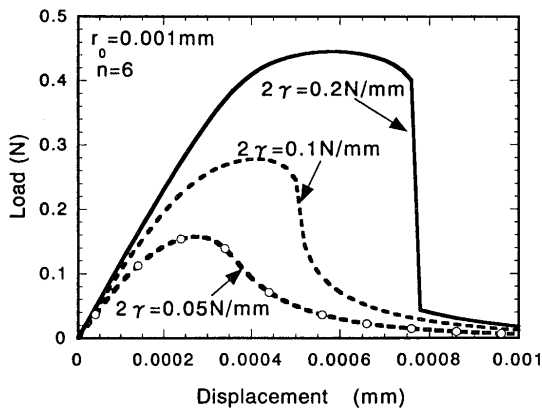


Fig.12 Load-displacement curve of push-out test.

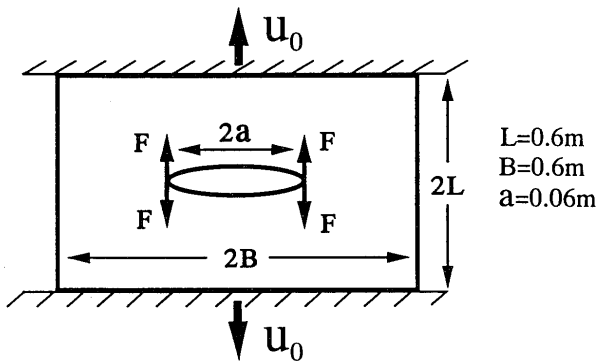


Fig.13 Model for dynamic crack propagation.

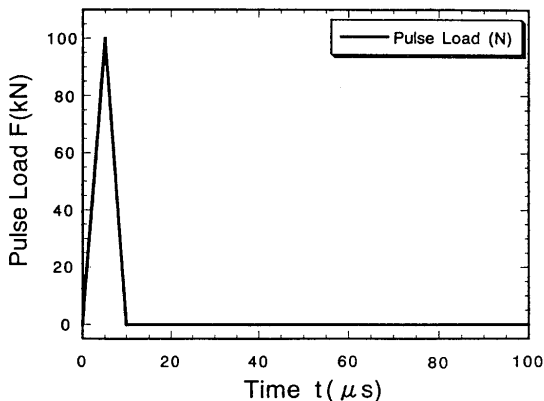


Fig.14 Pulse load to initiate crack propagation.

5. Dynamic Crack Propagation

In many cases, fracture problems are dynamic phenomena. To demonstrate the potential capability of the proposed method, the dynamic crack propagation in an elastic plate as shown in Fig.13 is analyzed. The plate has an initial crack with its length 400 mm and it is pre-stressed by the forced displacement at the top and the bottom edges. The crack is initiated by a pulse load applied at the tip of the initial crack. The pulse load increases and decreases linearly in $10 \mu\text{s}$ as shown in Fig.14. The time histories of crack extension lengths Δa for different values of pre-stress displacement u_0 are plotted in Fig.15. As theoretically predicted⁵⁾, the speed of crack propagation increases with the value of pre-stress. When the pre-stress is small as in the case of $u_0 = 0.4 \text{ mm}$, the crack is arrested. Figure 16 shows the crack extension and the stress distribution at 60 and 80 μs after the application of pulse load. Due to the symmetry, only left half of the plate is shown.

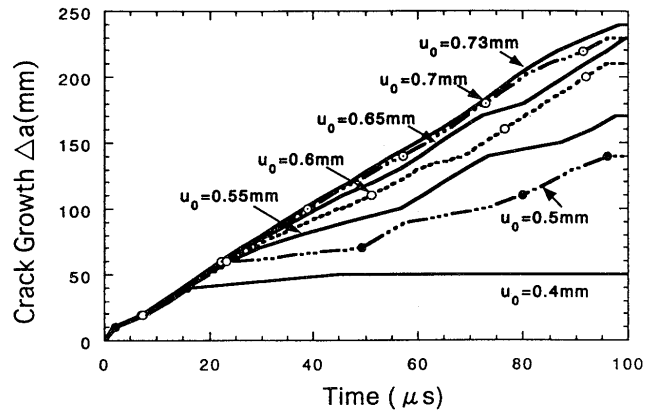


Fig.15 Influence of pre-stress on crack propagation length.

$2\gamma = 50 \text{ N/mm}$ $r_0 = 0.05 \text{ mm}$ $n = 6$
 $u_0 = 0.7 \text{ m}$ $\Delta t = 0.1 \mu\text{s}$ $a_0 = 60 \text{ mm}$

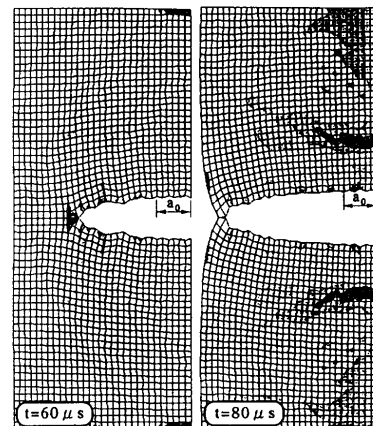


Fig.16 Deformation and Stress distribution during crack propagation.

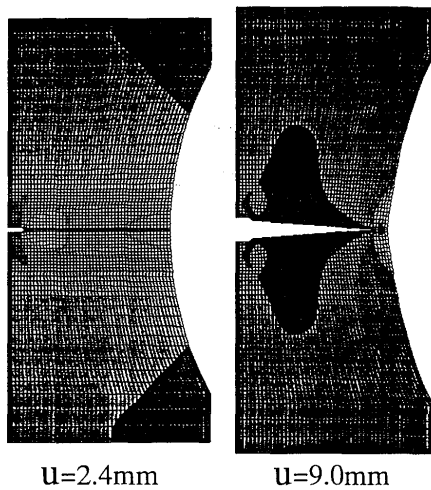


Fig.17 Deformation and stress distribution in tearing test.

6. Ductile Tearing of Steel Plate

The process of tearing of steel plate with an initial notch at its center is analyzed as an elastic-plastic finite strain problem using the proposed method. The length of the initial notch in the steel plate is 20 mm. The width of the plate at the center section and the thickness are 200 mm and 4.5 mm, respectively. The computed deformation and the distribution of the stress component in the loading direction before the crack propagation and at the final stage are presented in Fig.17. The curves for nominal stress-strain relation are compared between FEM analysis and experiment in Fig.18. The strain is the average strain for the 50 mm gauge length at the center. Good correlation between the computation and the experiment proves the potential capability of the proposed method for the analysis of ductile crack propagation.

7. Conclusions

In order to analyze crack propagation and peeling, a new computer simulation method using an interface element is proposed and applied to the peeling test of film, the push-out test of a fiber in matrix, a dynamic crack in pre-stressed plate and the ductile tearing of steel plate. The conclusions can be summarized as follows.

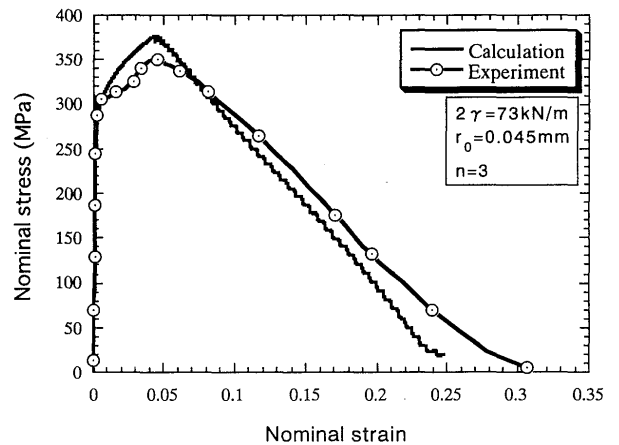


Fig.18 Comparison between theory and experiment.

- (1) The processes of mode-I and II crack propagation can be simulated by the proposed method.
- (2) In the simulation of the peeling test, the material constants r_0 and n influence the load at the beginning of crack propagation, but they do not influence the processes of crack propagation. On the other hand, γ influences both the beginning and the processes of crack propagation. The effect of mesh division on the crack propagation is found to be small.
- (3) The dynamic crack propagation in a pre-stressed elastic plate is simulated and the relation between the crack propagation speed and the pre-stress is clarified.
- (4) Good correlation with experiment proves the potential capability of the proposed method for ductile fracture problems.

References

- 1) H. Noguchi *et al.*, Trans. Japan Society of Mechanical Engineers, (A) Vol.63 (1997), No. 608, p.725 (in Japanese).
- 2) H. Murakawa and Z.Q. Wu, Proc. of the Kansai Society of Naval Architects, No.10 (May 1998), p.125 (in Japanese).
- 3) M. Horibe *et al.*, Proc. of Welding Structure Symposium '97, Osaka, Japan (Nov.17-18, 1997), p.363 (in Japanese).
- 4) H. Serizawa *et al.*, Materials Transactions, JIM, Vol.37, No.3 (1997), p.409.
- 5) F. Nilsson, Engineering Fracture Mechanics, No.8 (1994), p.397.
- 6) A. Rahman, Phys. Rev., Vol.136 (1964), No.2A, p.405.